ACS APPLIED MATERIALS & INTERFACES

Research Article

www.acsami.org

Influence of Surface States on the Evaluation of the Flat Band Potential of TiO_2

Hao Ge,[†] Hui Tian,[†] Yangen Zhou,[§] Shuyao Wu,[†] Daliang Liu,[†] Xianzhi Fu,[§] Xi-Ming Song,*[,†] Xicheng Shi,*[,‡] Xuxu Wang,*[,§] and Ning Li[⊥]

[†]Liaoning Key Laboratory for Green Synthesis and Preparative Chemistry of Advanced Materials, College of Chemistry, Liaoning University, Shenyang, 110036, People's Republic of China

[‡]Research Institute of Chemical Defense, Beijing 100083, People's Republic of China

[§]Research Institute of Photocatalysis, Fuzhou University, 523 Gong Ye Road, 350002 Fuzhou, People's Republic of China

[⊥]Department of Applied Chemistry, Harbin Institute of Technology, Harbin 150001, People's Republic of China

Supporting Information

ABSTRACT: Flat band potential (V_{fb}) is one of the most important physical parameters to study and understand semiconductor materials. However, the influence of surface states on the evaluating V_{fb} of titanium oxide (TiO_2) and other semiconductor materials through a Mott–Schottky plot is ignored. Our study indicated that the influence of surface states should be introduced into the corresponding equivalent circuit even when the kinetic process did not occur. Ignoring the influence of surface states would lead to an underestimation of the space charge capacitance. Our paper would be beneficial for accurate determination of V_{fb} of semiconductor materials. We anticipate that this preliminary study will open new perspectives in understanding the semiconductor–electrolyte interface.

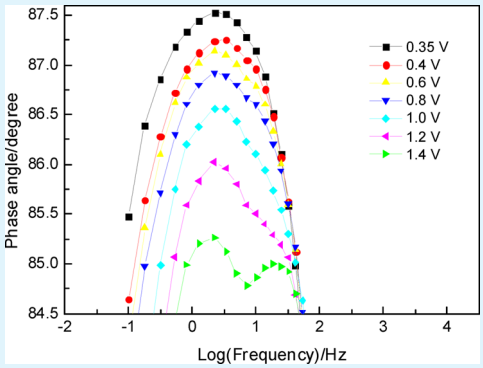

KEYWORDS: *Flat band potential, semiconductor materials, Mott–Schottky method, semiconductor–electrolyte interface, space charge capacitance, equivalent circuit*

INTRODUCTION

Semiconductor materials have been widely used and highly studied due to their unique character compared to conductor and insulator materials.[1−4] Particularly, TiO_2, with lots of excellent properties, has received great attention in environmental and energy applications, including catalysis, electrode material, water-splitting and photovoltaic conversion.[5−8] More than 10 000 publications on both fundamental and applied aspects are devoted to titanium oxide (TiO_2) every year. Electrochemical behaviors in the semiconductor–electrolyte interface are very important for understanding the performance of semiconductor materials in catalytic and other applications.[9−12] To analyze the electrochemical behaviors precisely, efficient equivalent circuits extracted from experimental results are indeed required because real semiconductor–electrolyte interface often deviates from ideal behavior.[13−17] Gerischer circuit elements are often used for describing the porous electrodes of batteries.[18] But the actual proof of the existence of the Gerischer impedance is observed much later.[19] The most direct derivation of the simplified Gerischer expression is via incorporating, according to Fick's second law.[20] Many studies have been performed to investigate the interfacial processes and especially the recombination/charge transfer mechanism.[21−24] However, the reasonable definition of equivalent circuits and the demonstration of processes occurring on electrodes are difficult due to the complexity of the system.[25] Recently, a number of works have highlighted the central role of surface states in the kinetic operation of hematite in water splitting conditions.[26−28] Bisquert formulated the kinetic model and provided a rigorous structure of the fundamental equivalent circuit including surface states for photoelectrochemical water splitting systems.[29]

Knowledge of the V_{fb} provides the first test that a material must pass to be a potentially effective photoelectrode or photocatalyst.[30] Consequently, there is an increasing need for accurate methods of determining band edge positions. Lots of methods have been developed for the determination of V_{fb}. The most often used method for the determination of V_{fb} is based on the measurement of the potential dependence of the space charge region capacity (C_{sc}), according to the Mott–Schottky relation.[31] The key of the Mott–Schottky method is to get actual values of C_{sc} at different applied potentials, which depends on an efficient equivalent circuit that can represent the real situation of semiconductor–electrolyte interface. Even

Received: October 26, 2013
Accepted: January 28, 2014
Published: January 28, 2014

   dx.doi.org/10.1021/am404743a | ACS Appl. Mater. Interfaces 2014, 6, 2401−2406

though the existence of surface states of semiconductor materials is generally recognized, the influence of surface states on the evaluation of the semiconductor−electrolyte interface capacitance and the V_{fb} through a Mott−Schottky plot is ignored. In this paper, the classical equivalent circuit for the evaluation of the V_{fb} of semiconductor materials was improved. To minimize the complexity of the studied system, we performed electrochemical experiments in aqueous solution without reactant additives in dark conditions at different anodizing potentials. An improved equivalent circuit was obtained through studying the electrochemical impedance spectroscopy (EIS) and cyclic voltammograms (CV) of TiO_2 at different anodizing potentials. Our paper clearly elucidates why the influence of surface states should be considered in the test potential range. Compared to the prevailing kinetic equivalent circuits, behavior of surface states was introduced into our modified equivalent circuit even when the kinetic process did not occur, which made the estimation of the V_{fb} of semiconductor materials more precisely. We anticipate that our preliminary study will open new perspectives in determining V_{fb} of semiconductor materials.

EXPERIMENTAL SECTION

The working electrode was fabricated by dropping a total of 5 mg of commercial rutile TiO_2 (40 nm, from Alfa Aesar Co.) on the FTO glass, and the resulting films (1.0 × 1.0 cm) were heated in air at 200 °C for 1 h to improve adhesion. The thickness of the resulting films was 2 μm, equal to the thickness of the mold.

The morphology of the working electrode (rutile layer) was examined with scanning electron microscopy (SEM, Hitachi, S-4700). X-ray diffraction (XRD) was performed on Rigaku D/MAX-RC X-ray diffractometer with Cu Kα_1 (45 kV, 50 mA, step size = 0.02°, 10° < 2θ < 80°) monochromated radiation in order to identify the crystalline phase of the working electrode (rutile layer).

Electrochemical measurements were carried out in a three electrode cell that was composed of a thin semiconductor film as a working electrode, a platinum plate as a counter electrode, and a saturated Ag/AgCl (3 M KCl) electrode as a reference electrode. The electrolyte was a 0.1 M Na_2SO_4(aq) solution without additives and was purged with nitrogen gas for 2 h prior to the measurements. EIS measurements were performed on Precision PARC workstation. The test potential ranged from open circuit potential to 2.0 V and the frequency ranged from 1 to 10 mHz. CV measurements were conducted with a BAS Epsilon workstation (BASi Co., USA). The electrodes were investigated between open circuit potential and 2.0 V at a scanning rate of 100 mV/s.

RESULTS AND DISCUSSION

Figure 1a and 1b show the SEM image and XRD patterns of the working electrode (rutile layer). As shown, the rutile layer, compact and homogeneous, was polycrystalline with primary features having dimensions of ~40 nm (Figure 1a). Any other phase such as anatase TiO_2 was not detected among the diffraction peaks of the rutile layer (Figure 1b). The well-defined and sharp peaks in the XRD patterns of the rutile layer confirmed its phase purity and degree of crystallinity.

To improve the classical equivalent circuit for the evaluation of the V_{fb} of semiconductor materials, the EIS of rutile TiO_2 at different anodizing potentials were studied. The impedance plots of rutile TiO_2 in 0.1 M Na_2SO_4 aqueous solution at different anodizing potentials (Figure 2) all seemed to be composed of a semicircle, which was generally considered as the representation of the space charge layer of semiconductor materials when no electrochemical reaction happened.[12,13]

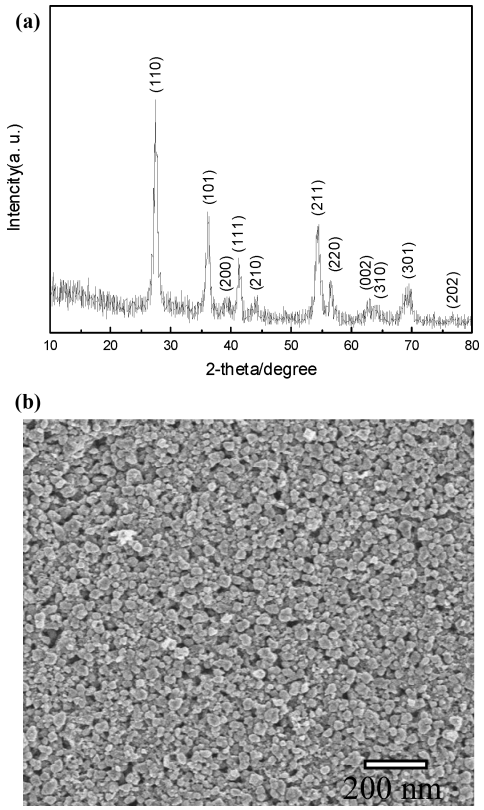

Figure 1. The SEM image (a) and X-ray diffraction (XRD) patterns (b) of the working electrode (rutile layer).

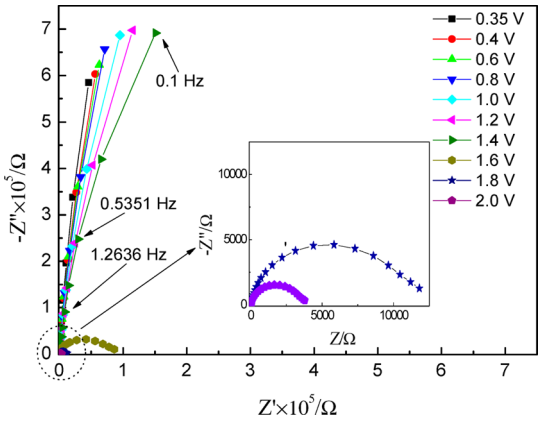

Figure 2. Impedance plots of rutile TiO_2 in 0.1 M Na_2SO_4 aqueous solution at different anodizing potentials.

Figure 3a,b displays the whole and local magnifying Bode plots of rutile TiO_2 in Na_2SO_4 aqueous solution at different anodizing potentials. As shown in Figure 3a, only one wide peak could be observed in each Bode plot at different anodizing potentials, which was in accordance with the results of Figure 2. However, to our surprise, Figure 3b showed a classical characteristic of two time constants.[32−34] Two peaks, more and more obvious with the positive shift of the anodizing potential, were detected in the local magnifying Bode plots of rutile TiO_2, suggesting that the semicircles of the corresponding impedance plots (Figure 2) were lapped by two semicircles indeed. Therefore, it was difficult to judge the number of semicircles of the investigated impedance plots and develop a reasonable equivalent circuit only from impedance plots. It

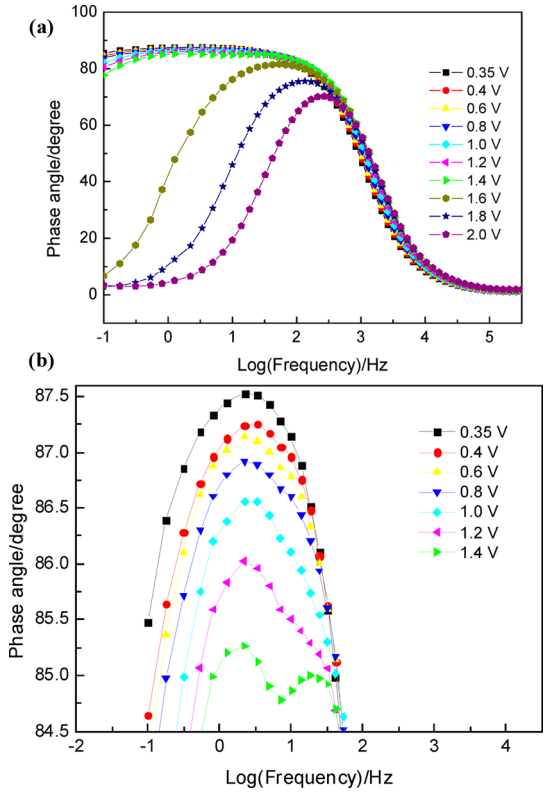

Figure 3. (a) Bode plots of rutile TiO_2 in 0.1 M Na_2SO_4 aqueous solution at different anodizing potentials; (b) local magnifying curves of panel a.

could be concluded that the equivalent circuit of the rutile TiO_2 in aqueous solution without reactant additives at different anodizing potentials was composed of two parts, not only the representation of space charge layer of semiconductor materials.

CV measurements were employed to study the electrochemical kinetics process. Figure 4 exhibits the CV curves of rutile TiO_2 in aqueous solution without reactant additives at different pH values. As shown in Figure 4, the weak current density could not be detected until the applied potential near to 2.0 V in 0.05 M H_2SO_4 aqueous solution. Therefore, the CV

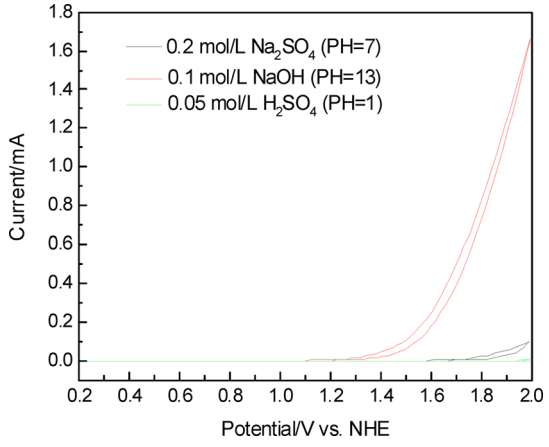

Figure 4. Cyclic voltammograms (CV) curves of rutile TiO_2 in aqueous solution without reactant additives at different pH values from the open circuit potential to 2.0 V.

measurements were performed from open circuit potentials to 2.0 V. The intensity of the detected reaction current enhanced remarkably from pH = 1 to 13. And with the pH value of electrolyte increasing from 7 to 13, the initial potential of the detected reaction current moved negatively about 0.5 V. The CV results suggested that electrochemical reaction could occur when there was no reactant additive in electrolyte and pH value of electrolyte had strong influence on the detected electrochemical reaction. During the CV measurements, an air bubble was observed on the surface of the working electrode and counter electrode at the initial potential of the detected reaction current. Because rutile TiO_2 and Na_2SO_4 were unable to be oxidized under the anodizing potentials (from open circuit potential to 2.0 V)[12−14] and there was no reactant additive in electrolyte, the air bubble observed on the surface of the working electrode and counter electrode was confirmed to be the oxidation and reduction production of H_2O. Accordingly, the reaction on the surface of the working electrode could be exhibited by formula 1.

$$2H_2O \rightarrow O_2 \uparrow + 4H^+ + 4e^- \quad (1)$$

As shown in formula 1, this reaction could be promoted and restrained in alkali and acid solution, which was confirmed with our CV results. The oxidation of H_2O to O_2 (formula 1) was allowed from the view of thermodynamic because the valence band of rutile TiO_2 was more positive than the reaction energy level of H_2O/O_2[9,35] (formula 1). According to previous studies,[23,24,26,36,37] charge transferred through surface states of the semiconductor materials when the electrochemical reactions occurred, charge-transfer processes (electrochemical reactions) were generally represented by surface states of semiconductor materials in the kinetics models. Consequently, the two parts of the equivalent circuit of our studied system were the space charge layer and surface states (charge-transfer processes) of semiconductor materials, respectively, when the anodizing potential was enough positive.

Moreover, a characteristic of two time constants could be observed in the spectra registered below the thermodynamic potential of the reaction of the water oxidation (see Figure 3b). No anodic reaction could occur at the potential lower than the thermodynamic potential, no matter the position of the valence band of the semiconductor materials. Although the oxygen evolution could not take place on the surface of working electrode until the anodizing potential was enough positive, there were surface states on the surface of any real semiconductor materials even if no charge-transfer process happened. Therefore, not only the space charge layer but also surface states of semiconductor materials should be taken into account at any applied potential when developing an efficient equivalent circuit that could represent the real situation of the semiconductor−electrolyte interface. The theory of the impedance of a semiconductor with surface states had been elaborated by Z. Hens.[23] According to that theory, semiconductor materials with surface states could be described by the equivalent circuit with two time constants, which was consistent with our experimental results.

Furthermore, the response of surface states of TiO_2 could be enhanced in alkaline solution because surface states had to be correlated with hydroxyl groups at the surface of TiO_2.[38] Figure 5 displays the Bode plots of rutile TiO_2 in 0.1 M NaOH aqueous solution at different applied potentials. As shown in Figure 5, compared with Figure 3a, two obvious peaks without local magnifying were observed as evidence, which attributed to

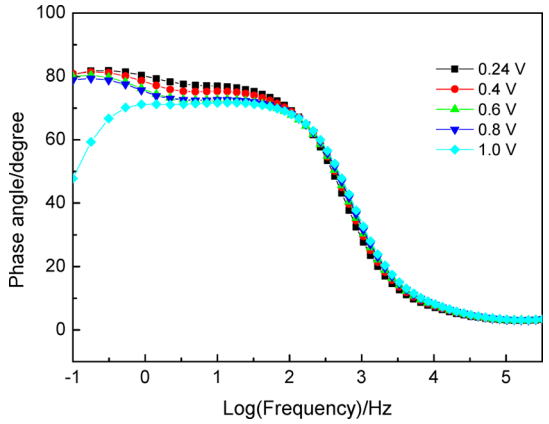

Figure 5. Bode plots of rutile TiO_2 in 0.1 M NaOH aqueous solution at different applied potentials.

the enhanced response of surface states of TiO_2 in alkaline. As shown in Figure 4, oxygen evolution could not occur when the applied potential below 1.1 and 1.6 V in alkaline and neutral solution; however, the corresponding Bode plots (Figures 5 and 3b) showed a classical characteristic of two time constants. Accordingly, except the space charge layer, the influence of the surface states of semiconductor materials on our studied system should also be considered when the electrochemical reaction (oxygen evolution) did not occur.

Figure 6 shows the improved (a) and classical (b) equivalent circuit of the proposed test system. R_S, C_{SS}, R_{SS}, C_{SC} and R_B

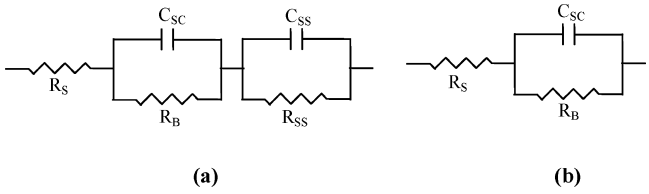

Figure 6. Modified (a) and classical (b) equivalent circuit of the proposed test system.

represent bulk electrolyte resistance, surface states capacitance, surface states resistance, space charge capacitance and bulk electrode resistance, respectively. Compared to the classical equivalent circuit for estimating V_{fb} of semiconductor materials, the existence of surface states was taken into account in our modified equivalent circuit. Moreover, the potential range of Mott–Schottky method was wide, in which it was assumed that the kinetic process did not occur. Consequently, the prevailing kinetic equivalent circuits[18,26,29] (proposed by Bisquert, Gerischer, Kelly, etc) were not suitable for Mott–Schottky method. Our study revealed that the influence of surface states should be introduced into the corresponding equivalent circuit even when the kinetic process did not happen, which would allow calculating the V_{fb} of semiconductor materials more accurately on the basement of our modified equivalent circuit.

One of the most important applications of the equivalent circuit for the semiconductor–electrolyte interface is in the measurement of the V_{fb} of semiconductor materials. Figure 7 presents the Mott–Schottky curves of rutile TiO_2 based on equivalent circuit (a) and (b). (Mott–Schottky curves of anatase TiO_2 and P25 based on equivalent circuit (a) and (b) are provided in the Supporting Information) As shown, the fitting parameters extracted from equivalent circuit (a)

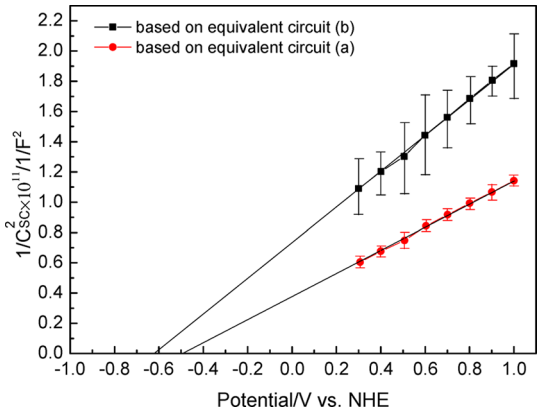

Figure 7. Mott–Schottky curves of rutile TiO_2 based on equivalent circuit (a) and (b).

exhibited a relative error of less than 2%, whereas those were higher than 10% on the basement of equivalent circuit (b). Figure 8 exhibits the fitted impedance and Bode curves extracted from classical equivalent circuit (panels a and c) and our improved equivalent circuit (panels b and d). As shown, the original Bode curves showed notable characteristic of two time constants. There were so many deviated points between experimental curves and the fitted curves extracted from the Figure 6b, contributing to the higher error of the fitting parameters extracted from the classical equivalent circuit. However, compared with the classical equivalent circuit, the fitted curves calculated from our modified equivalent circuit matched well with experimental curves, which attributed to the consideration of the surface states.

Further, as shown in Figure 7, the obtained values of C_{sc} at different applied potentials became big and the measured flat band potential moved positively about 0.14 V (0.09 and 0.11 V for anatase TiO_2 and P25, respectively, (see Figure S1 and Figure S2, Supporting Information)) when employing our improved equivalent circuit. The capacitance extracted from equivalent circuit (a) could be expressed by formula 2.

$$\frac{1}{C} = \frac{1}{C_{SC}} + \frac{1}{C_{SS}} \quad (2)$$

As shown in formula 2, a smaller value of C_{sc} would be obtained when the influence of surface states is ignored. Consequently, the value of C_{sc} extracted from equivalent circuit (b) was smaller than that calculated from equivalent circuit (a), which led to a more negative value for the determined V_{fb}. Obviously, ignoring the influence of surface states would result in departure of the obtained results from the actual values.

We also noticed that the information of our investigated system could not be extracted from the CV curves before the initial potential of the oxygen onset. However, EIS was sensitive even when the value of the detected current closed to zero, which demonstrated that the EIS was a powerful tool to study the surface states of semiconductor materials.

CONCLUSIONS

In summary, observation of two peaks in the Bode plots of rutile TiO_2 in aqueous solution without reactant additives at different anodizing potentials revealed that the influence of surface states should be considered in the corresponding equivalent circuit even when the kinetic process did not occur. Not only the space charge layer but also surface states of

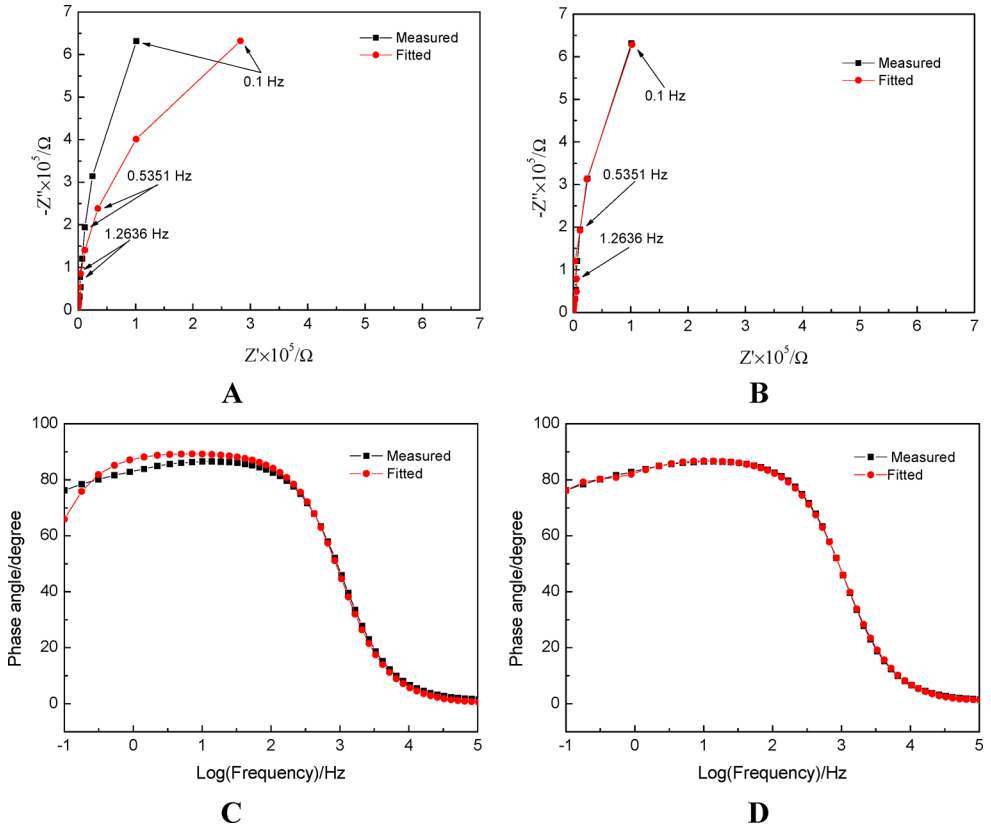

Figure 8. Fitted impedance and Bode curves extracted from classical equivalent circuit ((a) and (c)) and our improved equivalent circuit ((b) and (d)). The original curves were of the rutile TiO_2 in 0.1 M Na_2SO_4 aqueous solution at 0.4 V.

semiconductor materials should be taken into account at any applied potential when developing an efficient equivalent circuit that could represent the real situation of semiconductor–electrolyte interface. The contribution of surface states to the determination of the V_{fb} of semiconductor materials though Mott–Schottky plots could not be neglected. A more negative value for the determined V_{fb} would be acquired when ignoring the influence of surface states of semiconductor materials.

■ ASSOCIATED CONTENT

Supporting Information

Mott–Schottky curves of anatase TiO_2 and P25 based on equivalent circuit (a) and (b). This material is available free of charge via the Internet at http://pubs.acs.org.

■ AUTHOR INFORMATION

Corresponding Authors

*S. X. M. E-mail: songlab@lnu.edu.cn.
*S. X. C. E-mail: shxch163@163.com.
*W. X. X. E-mail: xwang@fzu.edu.cn.

Notes

The authors declare no competing financial interest.

■ ACKNOWLEDGMENTS

This work was supported by National Natural Science Foundation of China (51108455) and Science Foundation for Young Scholars of Liaoning University (2012LNDQN09).

■ REFERENCES

(1) Fujishima, A.; Honda, K. *Nature* **1972**, *238*, 37–38.
(2) Hoffma.n, M. R.; Martin, S. T.; Choi, W. *Chem. Rev.* **1995**, *95*, 69–96.
(3) Einaga, H.; Futamura, S.; Ibusuki, T. *Phys. Chem. Chem. Phys.* **1999**, *1*, 4903–4908.
(4) Potje-Kamloth, K. *Chem. Rev.* **2008**, *108*, 367–399.
(5) Thompson, T. L.; Yates, J. T. J. *Chem. Rev.* **2006**, *106*, 4428–4453.
(6) Osterloh, F. E. *Chem. Mater.* **2008**, *20*, 35–54.
(7) Burda, C.; Chen, X.; Narayanan, R.; El-Sayed, M. A. *Chem. Rev.* **2005**, *105*, 1025–1102.
(8) Chen, X.; Mao, S. S. *Chem. Rev.* **2007**, *107*, 2891–2959.
(9) Radecka, M.; Rekas, M.; Trenczek-Zajac, A.; Zakrzewska, K. *J. Power Sources* **2008**, *181*, 46–55.
(10) Jakob, M.; Levanon, H.; Kamat, P. V. *Nano Lett.* **2003**, *3*, 353–358.
(11) Röppischer, H.; Bumai, Y. A.; Feldmann, B. *J. Electrochem. Soc.* **1995**, *142*, 650–655.
(12) Kim, Y., II.; Atherton, S.; Brigham, E. S.; Mallouk, T. E. *J. Phys. Chem.* **1993**, *97*, 11802–11810.
(13) Spagnol, V.; Sutter, E.; Debiemme-Chouvy, C.; Cachet, H.; Baroux, B. *Electrochim. Acta* **2009**, *54*, 1228–1232.
(14) Ronga, I.; Bsiesy, A.; Gaspard, F.; Herino, R.; Ligeon, M.; Muller, F. *J. Electrochem. Soc.* **1991**, *138*, 3450–3456.
(15) Schlichthorl, G.; Peter, L. M. *J. Electrochem. Soc.* **1994**, *141*, L171–L173.
(16) Ottow, S.; Popkirov, G. S.; Foll, H. *J. Electroanal. Chem.* **1998**, *455*, 29–37.
(17) Cardon, F.; Gomes, W. P. *J. Phys. D: Appl. Phys.* **1978**, *11*, L63–L67.
(18) Jossen, A. *J. Power Sources* **2006**, *154*, 530–538.
(19) Makkus, R. C.; Hemmes, K.; Bunsenges, B. *Phys. Chem.* **1990**, *94*, 960–967.
(20) Boukamp, B. A.; Bouwmeester, H.J.M. *Solid State Ionics* **2003**, *157*, 29–31.

(21) Vanmaekelbergh, D.; Cardon, F. *J. Phys. D: Appl. Phys.* **1986**, *19*, 643−654.
(22) Ponomarev, E. A.; Peter, L. M. A. *J. Electroanal. Chem.* **1995**, *397*, 45−52.
(23) Hens, Z. *J. Phys. Chem. B* **1999**, *103*, 122−129.
(24) Leng, W. H.; Zhang, Z.; Zhang, J. Q.; Cao, C. N. *J. Phys. Chem. B* **2005**, *109*, 15008−15023.
(25) Wang, Q.; Gra1tzel, M. *J. Phys. Chem. B* **2005**, *109*, 14945−14953.
(26) Klahr, B.; Gimenez, S.; Fabregat-Santiago, F.; Hamann, T.; Bisquert, J. *J. Am. Chem. Soc.* **2012**, *134*, 4294−4302.
(27) Klahr, B.; Gimenez, S.; Fabregat-Santiago, F.; Bisquert, J.; Hamann, T. W. *Energy Environ. Sci.* **2012**, *5*, 7626−7636.
(28) Braun, A.; Sivula, K.; Bora, D. K.; Zhu, J.; Zhang, L.; Gratzel, M.; Guo, J. *J. Phys. Chem. C* **2012**, *116*, 16870−16875.
(29) Bertoluzzi, L.; Bisquert, J . *J. Phys. Chem. Lett.* **2012**, *3*, 2517−2522.
(30) Ondersma, J. W.; Hamann, T. W. *Energy Environ. Sci.* **2012**, *5*, 9476−9480.
(31) Chazalviel, J.-N. *Surf. Sci.* **1979**, *88*, 204−220.
(32) Pu, P.; Cachet, H.; Sutter, E. M. M. *Electrochim. Acta* **2010**, *55*, 5938−5946.
(33) Wang, Y. G.; Zhang, X. G. *Electrochim. Acta* **2004**, *49*, 1957−1962.
(34) Liu, H.; Cheng, S. A.; Wu, M.; Wu, H. J.; Zhang, J. Q.; Li, W. Z.; Cao, C. N. *J. Phys. Chem.* **2000**, *104*, 7016−7020.
(35) Jeffrey, M. B.; Mark, S. W. *J. Phys. Chem.* **1976**, *80*, 2641−2645.
(36) Morrison, S. R. *Electrochemistry at Semiconductor and Oxidized Metal Electrodes*; Plenum Press: New York, 1980.
(37) Vanmaekelbergh, D. *Electrochim. Acta* **1997**, *42*, 1121−1134.
(38) Antonio, A.; Derek, J. H.; Joël, T.; Sandeep, P.; Roberto, A.; Gerardino, D.; Giuseppe, V.; Simona, F.; Henry, J. S. *J. Am. Chem. Soc.* **2013**, *135*, 13538−13548.